Z. Angew. Math. Phys. 62 (2011), 1101–1116
© 2011 Springer Basel AG
0044-2275/11/061101-16
published online June 11, 2011
DOI 10.1007/s00033-011-0134-3

Zeitschrift für angewandte Mathematik und Physik ZAMP

On the uniform stress state inside an inclusion of arbitrary shape in a three-phase composite

X. Wang and X.-L. Gao

Abstract. The stress field inside a two-dimensional arbitrary-shape elastic inclusion bonded through an interphase layer to an infinite elastic matrix subjected to uniform stresses at infinity is analytically studied using the complex variable method in elasticity. Both in-plane and anti-plane shear loading cases are considered. It is shown that the stress field within the inclusion can be uniform and hydrostatic under remote constant in-plane stresses and can be uniform under remote constant anti-plane shear stresses. Both of these uniform stress states can be achieved when the shape of the inclusion, the elastic properties of each phase, and the thickness of the interphase layer are properly designed. Possible non-elliptical shapes of inclusions with uniform hydrostatic stresses induced by in-plane loading are identified and divided into three groups. For each group, two conditions that ensure a uniform hydrostatic stress state are obtained. One condition relates the thickness of the interphase layer to elastic properties of the composite phases, while the other links the remote stresses to geometrical and material parameters of the three-phase composite. Similar conditions are analytically obtained for enabling a uniform stress state inside an arbitrary-shape inclusion in a three-phase composite loaded by remote uniform anti-plane shear stresses.

Mathematics Subject Classification (2000). 74A40 · 74A50 · 74B05.

Keywords. Inclusion · Interphase · Uniform hydrostatic stress field · Plane elasticity · Anti-plane shear · Complex variable method · Conformal mapping · Harmonic inclusion.

1. Introduction

It is known that constant stresses at infinity will induce a uniform stress state inside an elastic inclusion perfectly bonded to an infinite elastic matrix when the inclusion has an elliptical or ellipsoidal shape and classical elasticity is used (e.g., [5,12,13,15,28]). However, the stress field inside an inclusion of non-elliptical or non-ellipsoidal shape is generally non-uniform. The Faber polynomials and Laurent series can be employed to determine the non-uniform stress field within a two-dimensional (2-D) inclusion of irregular shape (e.g., [7,14,23,28]).

Can the stress field in a non-elliptical or non-ellipsoidal inclusion be uniform when the inclusion/matrix interface is imperfect or when an interphase layer of finite thickness exists between the inclusion and the matrix? Antipov and Schiavone [1] have shown that the stress field within a non-elliptical inclusion imperfectly bonded to an infinite matrix with a spring–layer-type interface can still be uniform when the matrix is subjected to remote constant anti-plane shear stresses and when the imperfect interface is judiciously designed.

Ru [17] has demonstrated that a uniform hydrostatic stress state can be achieved inside an *elliptical* inclusion that is perfectly bonded to an infinite elastic matrix (loaded by uniform far-field stresses) through an interphase layer of finite thickness. Such uniform hydrostatic stress states are important for designing harmonic shapes, which is an inverse elasticity problem (e.g., [2,4,17,24,27]).

However, no work has been reported on how to achieve uniform hydrostatic stresses inside a *non-elliptical* inclusion when the matrix is subjected to remote in-plane stresses. This motivated the current study.

Birkhäuser

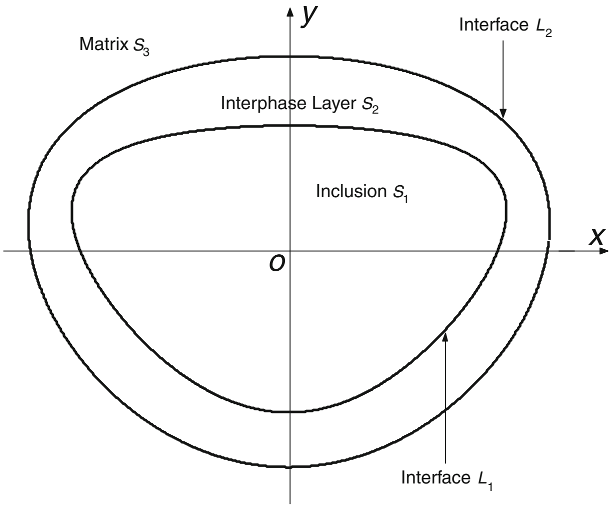

FIG. 1. Three-phase composite with an inclusion of arbitrary shape

In the present paper, the existence of a uniform hydrostatic stress state inside an arbitrary-shape (non-elliptical) inclusion bonded through an interphase layer to an infinite elastic matrix subjected to remote uniform in-plane stresses is shown. Possible non-elliptical inclusion shapes that enable such uniform hydrostatic stress states are identified and divided into three groups. For each group, two conditions are analytically obtained. One links the thickness of the interphase layer to elastic constants of the composite, while the other establishes a relation among the remote applied stresses, geometrical parameters and elastic properties of the three-phase composite. By following similar procedures, possible inclusion shapes and the related conditions for generating uniform stress fields inside inclusions under remote anti-plane shear stresses are also identified.

2. Formulation

Consider an arbitrary-shape elastic inclusion bonded to an infinite elastic matrix through an interphase layer, as shown in Fig. 1. Let S_1, S_2, and S_3 denote, respectively, the inclusion, the interphase layer, and the matrix. These three phases are perfectly bonded to each other at two interfaces L_1 and L_2. The matrix S_3 is subjected to uniform (constant) in-plane stresses $\sigma_{xx}^{\infty}, \sigma_{yy}^{\infty}$ and σ_{xy}^{∞} at infinity. Note that the subscript j or the superscript (j) will be used to indicate relevant quantities in region (phase) S_j in the sequel.

For plane deformations of an isotropic, linearly elastic material, the in-plane displacements u and v, stresses σ_{xx}, σ_{yy} and σ_{xy}, and resultant forces f_x and f_y of the tractions acting on an arbitrary boundary segment AB can be expressed in terms of two analytic functions $\phi(z)$ and $\psi(z)$ of the complex variable $z = x + iy$ as (e.g., [8,10,11,16,20])

$$\begin{aligned} 2\mu(u + iv) &= \kappa\phi(z) - z\overline{\phi'(z)} - \overline{\psi(z)}, \\ f_x + if_y &= -i[\phi(z) + z\overline{\phi'(z)} + \overline{\psi(z)}]_A^B, \end{aligned} \tag{1}$$

$$\begin{aligned} \sigma_{xx} + \sigma_{yy} &= 2[\phi'(z) + \overline{\phi'(z)}], \\ \sigma_{yy} - \sigma_{xx} + 2i\sigma_{xy} &= 2[\bar{z}\phi''(z) + \psi'(z)], \end{aligned} \tag{2}$$

where $\kappa = (3-\nu)/(1+\nu)$ for plane stress deformations or $\kappa = 3 - 4\nu$ for plane strain deformations (with the latter assumed in the current study), μ and ν (with $\mu > 0$ and $0 \le \nu \le 0.5$) are, respectively, the shear modulus and Poisson's ratio, and i is the usual imaginary number with $i^2 = -1$. Also, the overhead bar represents the conjugate, and the prime denotes the derivative with respect to z (e.g., $\phi'(z) = \mathrm{d}\phi/\mathrm{d}z, \phi''(z) = \mathrm{d}^2\phi/\mathrm{d}z^2$) here and throughout the paper.

2.1. Uniform hydrostatic stress state under in-plane loading

Consider the conformal mapping function (e.g., [6,21]):

$$z = \omega(\xi) = R\left(\xi + \sum_{n=1}^{N} \frac{a_n}{\xi^n}\right), \quad \xi = \omega^{-1}(z), \tag{3}$$

where ω is the transformation (or mapping) function from a complex variable ξ in the ξ-plane to the complex variable $z = x + iy$ in the physical z-plane, R is a real scaling constant, and $a_n (n = 1, 2, \ldots, N)$ are complex constants. This mapping function can conformally map the domain $S_2 \cup S_3$ in the z-plane onto the domain $|\xi| \ge 1$ in the ξ-plane. That is, the exterior of the inner interface curve L_1 in the z-plane is mapped onto the exterior of the unit circle $|\xi| = 1$ in the ξ-plane (see Fig. 2), with L_1 mapped to $|\xi| = 1$. Because the mapping function $\omega(\xi)$ in Eq. (3) is conformal (and thus one-to-one) for $|\xi| \ge 1$, one can design the thickness of the interphase layer S_2 enclosed by L_1 and L_2 in the z-plane such that the outer interface curve L_2 is mapped to $|\xi| = \rho^{-\frac{1}{2}}$, where ρ (with $0 < \rho < 1$) is a parameter measuring the relative thickness of S_2 in the physical plane. Clearly, $|\xi| = \rho^{-\frac{1}{2}}$(corresponding to L_2) is a circle co-axial with the smaller unit circle $|\xi| = 1$ (corresponding to L_1) in the ξ-plane (see Fig. 2). Several variants of the mapping function given in Eq. (3) have been used to study three-phase inclusion problems. For example, Ru and his co-workers [17,19] have investigated three-phase elliptical inclusion problems through using the mapping function $z = \omega(\xi) = R(\xi + \frac{1}{\xi})$, which is a special case of Eq. (3) with only the first two terms included, to map two confocal elliptical interfaces in the z-plane onto two co-axial circles in the ξ-plane. Very recently, Lu and Gao [14] have analyzed a three-phase coated inclusion problem by employing the mapping function of the same form as that given in Eq. (3) to map two closed, arbitrary-shape contours (as two surfaces of a coating of an inclusion) in the z-plane onto two concentric circles in the ξ-plane. Their analysis is based on the use of the Faber series.

With the use of Eq. (3), the physical regions S_2 and S_3 are mapped onto the circular regions $1 < |\xi| < \rho^{-\frac{1}{2}}$ and $|\xi| > \rho^{-\frac{1}{2}}$ in the ξ-plane, respectively. To ensure conformal mapping, it is required that $\omega'(\xi) \ne 0$ for any ξ in the domain $|\xi| > 1$. For simplicity, the following notation will be used interchangeably:

$$\phi_i(z) = \phi_i(\xi), \quad \psi_i(z) = \psi_i(\xi) \quad (i = 1, 2, 3). \tag{4}$$

In the ξ-plane, the traction and displacement continuities on the two interfaces of the three-phase composite can be expressed as

$$\left.\begin{aligned} &\phi_2(\xi) + \omega(\xi)\overline{\frac{\phi_2'(\xi)}{\omega'(\xi)}} + \overline{\psi_2(\xi)} = \phi_1(\xi) + \omega(\xi)\overline{\frac{\phi_1'(\xi)}{\omega'(\xi)}} + \overline{\psi_1(\xi)},\\ &\kappa_2\phi_2(\xi) - \omega(\xi)\overline{\frac{\phi_2'(\xi)}{\omega'(\xi)}} - \overline{\psi_2(\xi)} = \frac{\kappa_1}{\Gamma_1}\phi_1(\xi) - \frac{1}{\Gamma_1}\omega(\xi)\overline{\frac{\phi_1'(\xi)}{\omega'(\xi)}} - \frac{1}{\Gamma_1}\overline{\psi_1(\xi)} \end{aligned}\right\} \text{on } |\xi| = 1, \tag{5}$$

$$\left.\begin{aligned} &\phi_3(\xi) + \omega(\xi)\overline{\frac{\phi_3'(\xi)}{\omega'(\xi)}} + \overline{\psi_3(\xi)} = \phi_2(\xi) + \omega(\xi)\overline{\frac{\phi_2'(\xi)}{\omega'(\xi)}} + \overline{\psi_2(\xi)},\\ &\kappa_3\phi_3(\xi) - \omega(\xi)\overline{\frac{\phi_3'(\xi)}{\omega'(\xi)}} - \overline{\psi_3(\xi)} = \Gamma_3\kappa_2\phi_2(\xi) - \Gamma_3\omega(\xi)\overline{\frac{\phi_2'(\xi)}{\omega'(\xi)}} - \Gamma_3\overline{\psi_2(\xi)} \end{aligned}\right\} \text{on } |\xi| = \rho^{-\frac{1}{2}}, \tag{6}$$

where $\Gamma_1 \equiv \mu_1/\mu_2$ and $\Gamma_3 \equiv \mu_3/\mu_2$, as defined, are the shear modulus ratios. In addition, the boundary conditions of uniform applied stresses at infinity dictate that

$$\phi_3(\xi) \cong AR\xi + O(1), \quad \psi_3(\xi) \cong BR\xi + O(1) \quad \text{as} \quad |\xi| \to \infty, \tag{7a,b}$$

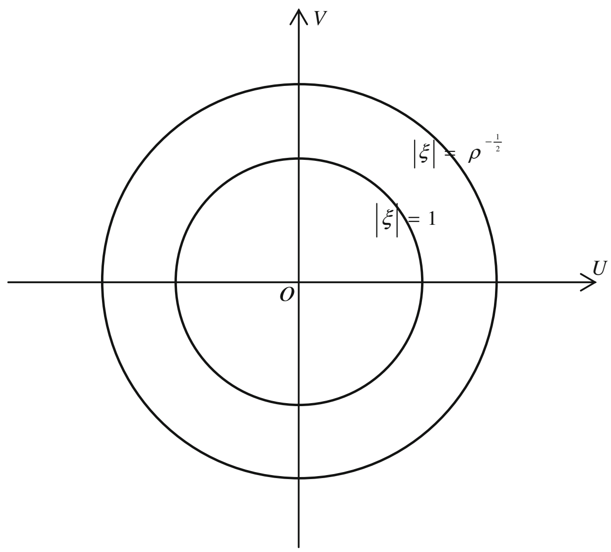

FIG. 2. Three-phase composite in the ξ-plane

where the constants A and B are determined from the remote constant stresses as

$$A = \frac{\sigma_{xx}^{\infty} + \sigma_{yy}^{\infty}}{4}, \quad B = \frac{\sigma_{yy}^{\infty} - \sigma_{xx}^{\infty} + 2i\sigma_{xy}^{\infty}}{2}, \tag{8}$$

assuming that there is no remote rigid-body rotation associated with the applied stresses.

Note that in reaching Eqs. (5) and (6) use has been made of Eqs. (1) and (4), and in obtaining Eqs. (7) and (8) use has been made of Eqs. (2) and (4). Also, "$O(1)$" in Eq. (7) is the usual big-Oh notation in asymptotic analysis, representing a constant.

For the stresses inside the inclusion S_1 to be uniform and hydrostatic, it follows from Eq. (2) that the two analytic functions $\phi_1(z)$ and $\psi_1(z)$ can be taken to be

$$\phi_1(z) = \frac{X}{R}z, \quad \psi_1(z) = 0, \tag{9}$$

where X is a real constant to be determined.

According to the analytic continuation method in the complex variable theory (e.g., [22]), Eq. (5) indicates that the two analytic functions $\phi_2(\xi)$ and $\psi_2(\xi)$ in the region $1 \le |\xi| \le \rho^{-\frac{1}{2}}$ can be expressed as

$$\phi_2(\xi) = \frac{\Gamma_1 + \kappa_1}{\Gamma_1(\kappa_2 + 1)}\phi_1(\xi) + \frac{\Gamma_1 - 1}{\Gamma_1(\kappa_2 + 1)}\left[\frac{\omega(\xi)}{\bar{\omega}'(1/\xi)}\bar{\phi}_1'(1/\xi) + \bar{\psi}_1(1/\xi)\right] \quad \left(1 \le |\xi| \le \rho^{-\frac{1}{2}}\right), \tag{10}$$

$$\psi_2(\xi) = \frac{\kappa_1 + 1}{1 - \Gamma_1}\bar{\phi}_1(1/\xi) - \frac{\Gamma_1\kappa_2 + 1}{1 - \Gamma_1}\bar{\phi}_2(1/\xi) - \frac{\bar{\omega}(1/\xi)}{\omega'(\xi)}\phi_2'(\xi) \quad \left(1 \le |\xi| \le \rho^{-\frac{1}{2}}\right). \tag{11}$$

Using Eqs. (10) and (11) in Eq. (6) results in the following two conditions on the interface $|\xi| = \rho^{-\frac{1}{2}}$:

$$\begin{aligned}\phi_3(\xi) = {} & \frac{\Gamma_3\kappa_2 + 1}{\kappa_3 + 1}\phi_2(\xi) - \frac{(1 - \Gamma_3)(\Gamma_1\kappa_2 + 1)}{(1 - \Gamma_1)(\kappa_3 + 1)}\phi_2(\rho\xi) \\ & + \frac{(1 - \Gamma_3)(\kappa_1 + 1)}{(1 - \Gamma_1)(\kappa_3 + 1)}\phi_1(\rho\xi) + \frac{1 - \Gamma_3}{\kappa_3 + 1}\frac{\omega(\xi) - \omega(\rho\xi)}{\bar{\omega}'\left(\frac{1}{\rho\xi}\right)}\bar{\phi}_2'\left(\frac{1}{\rho\xi}\right) \quad \text{on } |\xi| = \rho^{-\frac{1}{2}},\end{aligned} \tag{12}$$

$$\bar{\omega}\left(\frac{1}{\rho\xi}\right)\phi_3'(\xi)+\omega'(\xi)\psi_3(\xi)=\frac{\kappa_3-\Gamma_3\kappa_2}{\kappa_3+1}\omega'(\xi)\bar{\phi}_2\left(\frac{1}{\rho\xi}\right)+\frac{(\kappa_3+\Gamma_3)(\kappa_1+1)}{(1-\Gamma_1)(\kappa_3+1)}\omega'(\xi)\bar{\phi}_1\left(\frac{1}{\xi}\right)$$
$$-\frac{(\kappa_3+\Gamma_3)(\Gamma_1\kappa_2+1)}{(1-\Gamma_1)(\kappa_3+1)}\omega'(\xi)\bar{\phi}_2\left(\frac{1}{\xi}\right)+\frac{\kappa_3+\Gamma_3}{\kappa_3+1}\left[\bar{\omega}\left(\frac{1}{\rho\xi}\right)-\bar{\omega}\left(\frac{1}{\xi}\right)\right]\phi_2'(\xi)$$
$$\text{on } |\xi|=\rho^{-\frac{1}{2}}. \tag{13}$$

It can be shown that $\phi_3(\xi)$ and $\psi_3(\xi)$ to be obtained from Eqs. (12) and (13) will be analytic in the region $|\xi|>\rho^{-\frac{1}{2}}$ and satisfy the asymptotic conditions in Eqs. (7a,b) when

$$\phi_2(\xi)=\lambda\omega(\xi)\quad\left(1\le|\xi|\le\rho^{-\frac{1}{2}}\right), \tag{14}$$

where λ is a complex constant.

It should be mentioned that Eqs. (9) and (14) hold for the general case with $\Gamma_1\neq 1$ and $\Gamma_3\neq 1$. The special cases with $\Gamma_1=1$ and/or $\Gamma_3=1$ are separately discussed below.

Using Eqs. (9) and (3) in Eqs. (10) and (11) then yields

$$\phi_2(\xi)=\frac{X(2\Gamma_1+\kappa_1-1)}{\Gamma_1(\kappa_2+1)}\left(\xi+\sum_{n=1}^{N}\frac{a_n}{\xi^n}\right),\quad \psi_2(\xi)=\frac{2X\left[\Gamma_1(\kappa_2-1)+1-\kappa_1\right]}{\Gamma_1(\kappa_2+1)}\left(\frac{1}{\xi}+\sum_{n=1}^{N}\bar{a}_n\xi^n\right) \tag{15}$$

for $1<|\xi|<\rho^{-\frac{1}{2}}$. Substituting Eqs. (9) and (15) into Eqs. (12) and (13) and then using the analytic continuation method will lead to, with the help of Eq. (3),

$$\phi_3(\xi)=\frac{X(2\Gamma_1+\kappa_1-1)\left[\Gamma_3(\kappa_2-1)+2\right]}{\Gamma_1(\kappa_2+1)(\kappa_3+1)}\left(\xi+\sum_{n=1}^{N}\frac{a_n}{\xi^n}\right)$$
$$+\frac{2X(1-\Gamma_3)\left[\Gamma_1(\kappa_2-1)+1-\kappa_1\right]}{\Gamma_1(\kappa_2+1)(\kappa_3+1)}\left(\rho\xi+\sum_{n=1}^{N}\frac{a_n}{\rho^n\xi^n}\right),$$
$$\psi_3(\xi)=\frac{2X(2\Gamma_1+\kappa_1-1)\left[\Gamma_3(1-\kappa_2)+\kappa_3-1\right]}{\Gamma_1(\kappa_2+1)(\kappa_3+1)}\left(\frac{1}{\rho\xi}+\sum_{n=1}^{N}\bar{a}_n\rho^n\xi^n\right)$$
$$+\frac{2X(\Gamma_3+\kappa_3)\left[\Gamma_1(\kappa_2-1)+1-\kappa_1\right]}{\Gamma_1(\kappa_2+1)(\kappa_3+1)}\left(\frac{1}{\xi}+\sum_{n=1}^{N}\bar{a}_n\xi^n\right)$$
$$-\frac{2X(1-\Gamma_3)\left[\Gamma_1(\kappa_2-1)+1-\kappa_1\right]\left(\frac{1}{\rho\xi}+\sum_{n=1}^{N}\bar{a}_n\rho^n\xi^n\right)\left(\rho\xi-\sum_{n=1}^{N}\frac{na_n}{\rho^n\xi^n}\right)}{\Gamma_1(\kappa_2+1)(\kappa_3+1)\left(\xi-\sum_{n=1}^{N}\frac{na_n}{\xi^n}\right)} \tag{16}$$

for $|\xi|>\rho^{-\frac{1}{2}}$.

Clearly, $\phi_3(\xi)$ given in Eq. (16) satisfies the asymptotic conditions in Eq. (7a). For $\psi_3(\xi)$ in Eq. (16) to satisfy Eq. (7b), it has been found that the conformal mapping function $\omega(\xi)$ listed in Eq. (3) can take one of the following forms:

(a) $N=2$:

$$z=\omega(\xi)=R\left(\xi+\frac{a_1}{\xi}+\frac{a_2}{\xi^2}\right), \tag{17}$$

which was suggested in [24] for the design of harmonic shapes under non-uniform loading. As an example of this mapping function, Fig. 1 is drawn by taking $a_1=0.2, a_2=0.1i$ and $\rho=1/1.69$.

(b) $N=3$ with $a_2=0$:

$$z=\omega(\xi)=R\left(\xi+\frac{a_1}{\xi}+\frac{a_3}{\xi^3}\right), \tag{18}$$

which can be employed to approximate a rectangle (centered at origin with its sides parallel to the coordinate axes) (e.g., [18,25]) by taking $a_1 = (P + \bar{P})/2$ and $a_3 = (P - \bar{P})^2/24$, with $P = \mathrm{e}^{2ik\pi}$ where k is the aspect ratio of the rectangle.

(c) $N \geq 4$ with $a_1 = a_2 = \cdots = a_{N-1} = 0$:

$$z = \omega(\xi) = R\left(\xi + \frac{a_N}{\xi^N}\right) \quad (N \geq 4), \tag{19}$$

which can be adopted to describe a hypotrochoid by taking $0 \leq a_N \leq 1/N$ (e.g., [6,16]).

These three cases will be discussed in detail next.

Case (a) : $N = 2$

Using Eqs. (16) and (7a,b), along with Eqs. (17) and (3) for the conformal mapping function $z = \omega(\xi)$, gives, after comparing the coefficients of ξ and ξ^2,

$$\begin{aligned} AR &= \frac{X\left\{(2\Gamma_1 + \kappa_1 - 1)\left[\Gamma_3(\kappa_2 - 1) + 2\right] + 2\rho(1 - \Gamma_3)\left[\Gamma_1(\kappa_2 - 1) + 1 - \kappa_1\right]\right\}}{\Gamma_1(\kappa_2 + 1)(\kappa_3 + 1)}, \\ BR &= \frac{2\bar{a}_1 X\left\{\left[\Gamma_3 + \kappa_3 + \rho^2(\Gamma_3 - 1)\right]\left[\Gamma_1(\kappa_2 - 1) + 1 - \kappa_1\right] - \rho(2\Gamma_1 + \kappa_1 - 1)\left[\Gamma_3(\kappa_2 - 1) + 1 - \kappa_3\right]\right\}}{\Gamma_1(\kappa_2 + 1)(\kappa_3 + 1)}, \\ &\rho^2(2\Gamma_1 + \kappa_1 - 1)\left[\Gamma_3(\kappa_2 - 1) + 1 - \kappa_3\right] - \left[\Gamma_3 + \kappa_3 + \rho^3(\Gamma_3 - 1)\right]\left[\Gamma_1(\kappa_2 - 1) + 1 - \kappa_1\right] = 0. \end{aligned} \tag{20a–c}$$

Solving Eq. (20c), which is a cubic equation in ρ, yields the values of ρ for given material properties. With ρ determined, Eqs. (20a,b) can then be solved to obtain

$$\begin{aligned} X &= \frac{R\Gamma_1(\kappa_2 + 1)(\kappa_3 + 1)(\sigma_{xx}^\infty + \sigma_{yy}^\infty)}{4(2\Gamma_1 + \kappa_1 - 1)\left[\Gamma_3(\kappa_2 - 1) + 2\right] + 8\rho(1 - \Gamma_3)\left[\Gamma_1(\kappa_2 - 1) + 1 - \kappa_1\right]}, \\ \bar{a}_1 f(\rho) &= \frac{\sigma_{yy}^\infty - \sigma_{xx}^\infty + 2i\sigma_{xy}^\infty}{\sigma_{xx}^\infty + \sigma_{yy}^\infty}, \end{aligned} \tag{21a,b}$$

where

$$f(\rho) \equiv \frac{\left[\Gamma_3 + \kappa_3 + \rho^2(\Gamma_3 - 1)\right]\left[\Gamma_1(\kappa_2 - 1) + 1 - \kappa_1\right] - \rho(2\Gamma_1 + \kappa_1 - 1)\left[\Gamma_3(\kappa_2 - 1) + 1 - \kappa_3\right]}{(2\Gamma_1 + \kappa_1 - 1)\left[\Gamma_3(\kappa_2 - 1) + 2\right] + 2\rho(1 - \Gamma_3)\left[\Gamma_1(\kappa_2 - 1) + 1 - \kappa_1\right]}. \tag{22}$$

The other parameter a_2 involved in the conformal mapping function given in Eq. (17) can be chosen arbitrarily provided that it satisfies the conformal mapping requirement of $\omega'(\xi) \neq 0$ (i.e., $\xi^3 - a_1\xi - 2a_2 \neq 0$ from Eq. (17)) for $|\xi| > 1$. The case with a_1 being real and a_2 being imaginary was discussed in [24]. It should also be mentioned that for the three-phase elliptical inclusion problem the parameter ρ can be chosen arbitrarily [17], while for the current three-phase arbitrary-shape inclusion problem ρ has to be determined from Eq. (20c).

Case (b) : $N = 3$ *with* $a_2 = 0$

Using Eqs. (16) and (7a,b), along with Eqs. (18) and (3) for the conformal mapping function $z = \omega(\xi)$, gives, after comparing the coefficients of ξ and ξ^3,

$$\begin{aligned} AR &= \frac{X\left\{(2\Gamma_1 + \kappa_1 - 1)\left[\Gamma_3(\kappa_2 - 1) + 2\right] + 2\rho(1 - \Gamma_3)\left[\Gamma_1(\kappa_2 - 1) + 1 - \kappa_1\right]\right\}}{\Gamma_1(\kappa_2 + 1)(\kappa_3 + 1)}, \\ BR &= \frac{2X\begin{pmatrix}\left\{\bar{a}_1(\Gamma_3 + \kappa_3) + \rho^2(\Gamma_3 - 1)\left[\bar{a}_1 - a_1\bar{a}_3(1 - \rho^2)\right]\right\}\left[\Gamma_1(\kappa_2 - 1) + 1 - \kappa_1\right] \\ -\bar{a}_1\rho(2\Gamma_1 + \kappa_1 - 1)\left[\Gamma_3(\kappa_2 - 1) + 1 - \kappa_3\right]\end{pmatrix}}{\Gamma_1(\kappa_2 + 1)(\kappa_3 + 1)}, \\ &\rho^3(2\Gamma_1 + \kappa_1 - 1)\left[\Gamma_3(\kappa_2 - 1) + 1 - \kappa_3\right] - \left[\Gamma_3 + \kappa_3 + \rho^4(\Gamma_3 - 1)\right]\left[\Gamma_1(\kappa_2 - 1) + 1 - \kappa_1\right] = 0. \end{aligned} \tag{23a–c}$$

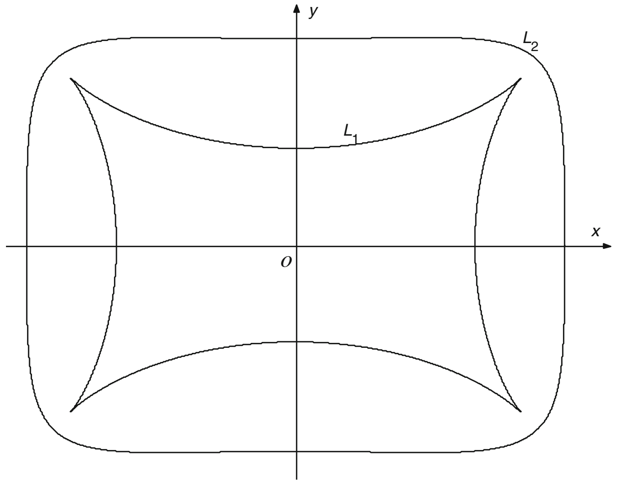

FIG. 3. Two interfaces L_1 and L_2 described by the conformal mapping function $z = R\left(\xi + \frac{a_1}{\xi} + \frac{a_3}{\xi^3}\right)$ with $a_1 = 0.2$, $a_3 = -1/3$ and $\rho = 1/1.69$

Solving Eq. (23c), a quartic equation in ρ, yields the values of ρ for given material properties. With ρ determined, Eqs. (23a,b) then give

$$X = \frac{R\Gamma_1(\kappa_2+1)(\kappa_3+1)(\sigma_{xx}^\infty+\sigma_{yy}^\infty)}{4(2\Gamma_1+\kappa_1-1)\left[\Gamma_3(\kappa_2-1)+2\right]+8\rho(1-\Gamma_3)\left[\Gamma_1(\kappa_2-1)+1-\kappa_1\right]}, \quad (24a)$$

$$\bar{a}_1 f(\rho) + a_1\bar{a}_3 g(\rho) = \frac{\sigma_{yy}^\infty - \sigma_{xx}^\infty + 2i\sigma_{xy}^\infty}{\sigma_{xx}^\infty + \sigma_{yy}^\infty}, \quad (24b)$$

where $f(\rho)$ is given in Eq. (22), and $g(\rho)$ is defined by

$$g(\rho) = \frac{\rho^2(1-\rho^2)(1-\Gamma_3)\left[\Gamma_1(\kappa_2-1)+1-\kappa_1\right]}{(2\Gamma_1+\kappa_1-1)\left[\Gamma_3(\kappa_2-1)+2\right]+2\rho(1-\Gamma_3)\left[\Gamma_1(\kappa_2-1)+1-\kappa_1\right]}. \quad (25)$$

For given remote stresses and material constants, Eq. (24b) provides a relation between the two geometrical parameters a_1 and a_3. In addition, a_1 and a_3 must satisfy the conformal mapping requirement of $\omega'(\xi) \neq 0$ (i.e., $\xi^4 - a_1\xi^2 - 3a_3 \neq 0$ from Eq. (18)) for $|\xi| > 1$. This is equivalent to requiring that $|a_1 \pm \sqrt{a_1^2 + 12a_3}| \leq 2$, which follows from evaluating the roots of the equation $\xi^4 - a_1\xi^2 - 3a_3 = 0$(quadratic in ξ^2) and requiring each root not to be outside the circle $|\xi| = 1$.

Figure 3 shows the shapes of the two interfaces L_1 and L_2 given by Eq. (18) with $a_1 = 0.2, a_3 = -1/3$, and $\rho = 1/1.69$. Note that the chosen values of a_1 and a_3 satisfy $|a_1 \pm \sqrt{a_1^2 + 12a_3}| = 2$ (rather than the inequality), giving $\omega'(\xi) = 0$ or $\xi^4 - a_1\xi^2 - 3a_3 = 0$. This explains the appearance of the four sharp corners on L_1 in Fig. 3, which correspond to the four roots of $\xi^4 - a_1\xi^2 - 3a_3 = 0$ that are located on the unit circle $|\xi| = 1$ on the ξ-plane.

Case (c) : $N \geq 4$ *with* $a_1 = a_2 = \cdots = a_{N-1} = 0$

Using Eqs. (16) and (7a,b), along with Eqs. (19) and (3) for the conformal mapping function $z = \omega(\xi)$, gives, after comparing the coefficients of ξ and ξ^N,

$$\sigma_{xx}^\infty = \sigma_{yy}^\infty = \frac{2X\left\{(2\Gamma_1+\kappa_1-1)\left[\Gamma_3(\kappa_2-1)+2\right]+2\rho(1-\Gamma_3)\left[\Gamma_1(\kappa_2-1)+1-\kappa_1\right]\right\}}{R\Gamma_1(\kappa_2+1)(\kappa_3+1)}, \quad \sigma_{xy}^\infty = 0,$$
$$\rho^N(2\Gamma_1+\kappa_1-1)\left[\Gamma_3(\kappa_2-1)+1-\kappa_3\right]-\left[\Gamma_3+\kappa_3+\rho^{N+1}(\Gamma_3-1)\right]\left[\Gamma_1(\kappa_2-1)+1-\kappa_1\right]=0. \quad (26)$$

Equation (26) shows that in this case the remote uniform stresses can only be hydrostatic.

Table 1. *Values of ρ when $\nu_1 = \nu_2 = \nu_3 = 1/3$*

	$N = 2$	$N = 3$	$N = 4$	$N = 5$	$N = 10$	$N = 20$
$\Gamma_1 = 0.9, \Gamma_3 = 0.1$	0.2805	0.4277	0.5283	0.5999	0.7740	0.8796
$\Gamma_1 = 0.8, \Gamma_3 = 0.4$	0.5386	0.6598	0.7310	0.7777	0.8811	0.9384
$\Gamma_1 = 2, \Gamma_3 = 5$	0.6436	0.7523	0.8108	0.8472	0.9222	0.9608
$\Gamma_1 = 1.2, \Gamma_3 = 10$	0.2936	0.4432	0.5441	0.6151	0.7852	0.8864

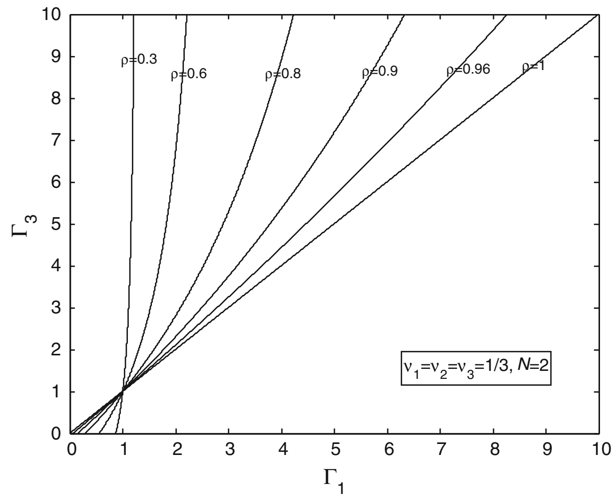

Fig. 4. Permissible Γ_1 and Γ_3 for given values of ρ with $\nu_1 = \nu_2 = \nu_3 = 1/3$ and $N = 2$

Note that in all of the three cases discussed above, ρ cannot be arbitrarily chosen for given material parameters $\Gamma_1, \Gamma_3, \kappa_1, \kappa_2$, and κ_3. This means that the "thickness" of the interphase layer has to be properly designed. In fact, ρ (with $0 \leq \rho \leq 1$) has to be determined from the following equation:

$$\rho^N (2\Gamma_1 + \kappa_1 - 1)\left[\Gamma_3(\kappa_2 - 1) + 1 - \kappa_3\right] - \left[\Gamma_3 + \kappa_3 + \rho^{N+1}(\Gamma_3 - 1)\right]\left[\Gamma_1(\kappa_2 - 1) + 1 - \kappa_1\right] = 0 \quad (27)$$

for $N \geq 2$. Equation (27) represents Eqs. (20c), (23c), and (26) when $N = 2, 3$, and ≥ 4, respectively.

Let the left-hand side of Eq. (27) be denoted by $h(\rho)$. Then, it can be readily shown that when $\frac{\mu_2}{\kappa_2-1} < \frac{\mu_1}{\kappa_1-1} < \frac{\mu_3}{\kappa_3-1}$ or $\frac{\mu_2}{\kappa_2-1} > \frac{\mu_1}{\kappa_1-1} > \frac{\mu_3}{\kappa_3-1}$, there is $h(0)h(1) < 0$, thereby ensuring the existence of one value of ρ on the interval $0 < \rho < 1$ as the root of Eq. (27). For a range of material properties satisfying the conditions identified above, the numerical analysis further shows that Eq. (27) gives a unique value of ρ on $0 \leq \rho \leq 1$. For example, when $\nu_1 = \nu_2 = \nu_3 = 1/3$, the values of ρ obtained from solving Eq. (27) for four different combinations of Γ_1 and Γ_3 are listed in Table 1. From this table, it is seen that ρ is an increasing function of N for fixed values of Γ_1 and Γ_3. This implies that the interphase layer becomes thinner as N increases (see Fig. 2).

Figure 4 illustrates the permissible Γ_1 and Γ_3 satisfying Eq. (27) for given values of ρ when $\nu_1 = \nu_2 = \nu_3 = 1/3$ and $N = 2$. It is clearly observed from Fig. 4 that for the given material parameters, the value of ρ determined from Eq. (27) is unique for both $\Gamma_3 > \Gamma_1 > 1$ and $\Gamma_3 < \Gamma_1 < 1$.

For a properly designed interphase, the uniform hydrostatic stresses inside the inclusion can be readily obtained from Eqs. (9) and (2), along with Eqs. (3) and (17), (18) or (19), as

$$\sigma_{xx}^{(1)} = \sigma_{yy}^{(1)} = \frac{2X}{R}, \quad \sigma_{xy}^{(1)} = 0; \quad \phi_1(z) = \frac{X}{R}z, \quad \psi_1(z) = 0 \ (z \in S_1), \quad (28)$$

where X is given in Eq. (21a) for $N = 2$, in Eq. (24a) for $N = 3$, or in Eq. (26) for $N \geq 4$.

In addition, it follows from Eqs. (2) and (15) that the mean stress is uniformly distributed in the interphase layer as

$$\sigma_{xx}^{(2)} + \sigma_{yy}^{(2)} = \frac{4X(2\Gamma_1 + \kappa_1 - 1)}{R\Gamma_1(\kappa_2 + 1)} \quad (z \in S_2). \tag{29}$$

Also, from Eqs. (28) and (29) and the relation $\sigma_{xx}^{(2)} + \sigma_{yy}^{(2)} = \sigma_{nn}^{(2)} + \sigma_{tt}^{(2)}$(i.e., the first stress invariant in plane deformations, with σ_{nn} and σ_{tt} being the radial and tangential stresses, respectively), the tangential (hoop) stress is constant along the entire interface L_1 (on the interphase layer side) and is given by

$$\sigma_{tt}^{(2)} = \frac{2X\left[\Gamma_1(3-\kappa_2) + 2(\kappa_1 - 1)\right]}{R\Gamma_1(\kappa_2 + 1)} \quad (z \in L_1). \tag{30}$$

Note that having a constant hoop stress on an interface or a hole boundary is very desirable in a stress minimization design (e.g., [2,4,17,24,26,27]). For instance, the hoop stress along the inner interface L_1 in Fig. 3 can be designed to be constant even though there are four sharp corners on L_1 (noting that sharp corners are usually locations of stress concentration or even stress singularity). In fact, an arbitrary-shape inclusion, which is directly bonded to a surrounding matrix (in the absence of an interphase layer), can be designed to be *harmonic* (see Appendix A for a brief discussion).

The specific expressions of $\phi_3(\xi)$ and $\psi_3(\xi)$ for the three cases can be obtained from Eqs. (16)–(19) and (3) once ρ, X, and a_N are determined or identified. These are presented in Appendix B.

It should be pointed out that when the three phases are all incompressible with $\nu_1 = \nu_2 = \nu_3 = 1/2$ (and thus $\kappa_1 = \kappa_2 = \kappa_3 = 1$ for plane strain deformations considered here) or when $\Gamma_1 = (\kappa_1 - 1)/(\kappa_2 - 1)$ and $\Gamma_3 = (\kappa_3 - 1)/(\kappa_2 - 1)$ with $\nu_2 \neq 1/2$, Eq. (27) is identically satisfied for any possible value of ρ on the interval $0 \leq \rho \leq 1$, and $f(\rho) = g(\rho) \equiv 0$ according to Eqs. (22) and (25). As a result, for all of the three cases discussed above, the remote uniform stresses can only be hydrostatic with $\sigma_{xx}^{\infty} = \sigma_{yy}^{\infty} = 2X/R, \sigma_{xy}^{\infty} = 0$, which follows from Eqs. (21b), (24b), (2)–(4), and (16).

It can be shown that the forms of the two analytic functions in the inclusion given in Eq. (9), which are obtained for the general case with $\Gamma_1 \neq 1$ and $\Gamma_3 \neq 1$ and ensure a uniform hydrostatic stress state inside the arbitrary-shape (non-elliptical) inclusion in the three-phase composite, are also valid for the two special cases with $\Gamma_1 = 1, \Gamma_3 \neq 1$ and $\Gamma_1 \neq 1, \Gamma_3 = 1$.

It follows from Eq. (27) that when $\Gamma_1 = 1, \Gamma_3 \neq 1$, the thickness parameter of the interphase layer, ρ, is defined by

$$\rho^N(1+\kappa_1)\left[\Gamma_3(\kappa_2 - 1) + 1 - \kappa_3\right] - \left[\Gamma_3 + \kappa_3 + \rho^{N+1}(\Gamma_3 - 1)\right](\kappa_2 - \kappa_1) = 0 \tag{31}$$

and when $\Gamma_1 \neq 1, \Gamma_3 = 1$ the thickness parameter ρ is explicitly given by

$$\rho = \left[\frac{(\kappa_3 + 1)\left[\Gamma_1(\kappa_2 - 1) + 1 - \kappa_1\right]}{(\kappa_2 - \kappa_3)(2\Gamma_1 + \kappa_1 - 1)}\right]^{\frac{1}{N}} \ (N \geq 2). \tag{32}$$

However, for the special case with $\Gamma_1 = \Gamma_3 = 1$, the two analytic functions in the inclusion S_1 no longer have the same forms as those given in Eq. (9), where $\psi_1(\xi) \equiv 0$. Consequently, the analytic functions in the interphase layer S_2 and in the matrix S_3 will also be different, as shown next.

2.1.1. Three phases with the same shear modulus: A special case. When the three phases have the same value of shear modulus, $\Gamma_1 = \Gamma_3 = 1$ and the two analytic functions in the inclusion can be expressed as

$$\phi_1(z) = \frac{X}{R}z, \quad \psi_1(z) = \frac{Y}{R}z, \tag{33}$$

where X is a real constant, and Y is a complex constant to be determined. After enforcing the continuity conditions of tractions and displacements across $|\xi| = 1$ and $|\xi| = \rho^{-\frac{1}{2}}$and using the analytic continuation method, the analytic functions in the interphase and in the matrix can be obtained as

$$\left.\begin{aligned} \phi_2(\xi) &= \tfrac{X(\kappa_1+1)}{\kappa_2+1}\left(\xi + \sum_{n=1}^{N} \tfrac{a_n}{\xi^n}\right), \\ \psi_2(\xi) &= \tfrac{2X(\kappa_2-\kappa_1)}{\kappa_2+1}\left(\tfrac{1}{\xi} + \sum_{n=1}^{N} \bar{a}_n \xi^n\right) + Y\left(\xi + \sum_{n=1}^{N} \tfrac{a_n}{\xi^n}\right) \end{aligned}\right\} \quad \left(1 < |\xi| < \rho^{-\frac{1}{2}}\right), \tag{34}$$

$$\left.\begin{aligned} \phi_3(\xi) &= \tfrac{X(\kappa_1+1)}{\kappa_3+1}\left(\xi + \sum_{n=1}^{N} \tfrac{a_n}{\xi^n}\right), \\ \psi_3(\xi) &= \tfrac{2X(\kappa_1+1)(\kappa_3-\kappa_2)}{(\kappa_2+1)(\kappa_3+1)}\left(\tfrac{1}{\rho\xi} + \sum_{n=1}^{N} \bar{a}_n \rho^n \xi^n\right) \\ &\quad + \tfrac{2X(\kappa_2-\kappa_1)}{\kappa_2+1}\left(\tfrac{1}{\xi} + \sum_{n=1}^{N} \bar{a}_n \xi^n\right) + Y\left(\xi + \sum_{n=1}^{N} \tfrac{a_n}{\xi^n}\right) \end{aligned}\right\} \quad \left(|\xi| > \rho^{-\frac{1}{2}}\right). \tag{35}$$

In order to satisfy the remote asymptotic conditions in Eq.(7), the conformal mapping function $\omega(\xi)$ defined in Eq. (3) needs to have the following form:

$$\omega(\xi) = R\left(\xi + \frac{a_1}{\xi} + \frac{a_N}{\xi^N}\right) \quad (N \geq 2). \tag{36}$$

By following a procedure similar to that used earlier for the general case with $\Gamma_1 \neq 1$ and $\Gamma_3 \neq 1$, the thickness parameter ρ for the current case can be determined to be

$$\rho = \left[\frac{(\kappa_3+1)(\kappa_1-\kappa_2)}{(\kappa_1+1)(\kappa_3-\kappa_2)}\right]^{\frac{1}{N}} (N \geq 2). \tag{37}$$

To ensure that ρ determined from Eq. (37) satisfies the condition of $0 \leq \rho \leq 1$, it is required that

$$\kappa_2 < \kappa_1 < \kappa_3 \quad \text{or} \quad \kappa_2 > \kappa_1 > \kappa_3, \tag{38}$$

which places a constraint on κ_1, κ_2, and κ_3 (and thus on Poisson's ratios ν_1, ν_2, and ν_3).

Along with Eqs. (37) and (38), the two constants X and Y can be determined from Eqs. (35), (7a,b), (8), (3), and (36) as

$$\begin{aligned} X &= \frac{R(\kappa_3+1)(\sigma_{xx}^{\infty}+\sigma_{yy}^{\infty})}{4(\kappa_1+1)}, \\ Y &= \frac{R(\sigma_{yy}^{\infty}-\sigma_{xx}^{\infty}+2i\sigma_{xy}^{\infty})}{2} + \frac{\bar{a}_1 R(\sigma_{xx}^{\infty}+\sigma_{yy}^{\infty})(\kappa_1-\kappa_2)(\kappa_3+1)(1-\rho^{1-N})}{2(\kappa_1+1)(\kappa_2+1)}. \end{aligned} \tag{39}$$

This indicates that the uniform stresses within the inclusion are now unconditional (i.e., there is no restriction on the remote constant stresses to be applied).

In the physical z-plane, the analytic functions presented in Eqs. (34) and (35) for the special case with $\Gamma_1 = \Gamma_3 = 1$ can be expressed as, with the help of Eq. (4),

$$\left.\begin{aligned} \phi_2(z) &= \tfrac{X(\kappa_1+1)}{R(\kappa_2+1)} z, \\ \psi_2(z) &= \tfrac{2X(\kappa_2-\kappa_1)}{\kappa_2+1}\left\{\tfrac{1}{\xi(z)} + \bar{a}_1 \xi(z) + \bar{a}_N [\xi(z)]^N\right\} + \tfrac{Y}{R} z \end{aligned}\right\} \quad (z \in S_2), \tag{40}$$

$$\left.\begin{aligned} \phi_3(z) &= \tfrac{X(\kappa_1+1)}{R(\kappa_3+1)} z, \\ \psi_3(z) &= \tfrac{2X(\kappa_1+1)(\kappa_3-\kappa_2)}{(\kappa_2+1)(\kappa_3+1)}\left[\tfrac{1}{\rho\xi(z)} + \bar{a}_1 \rho \xi(z)\right] \\ &\quad + \tfrac{2X(\kappa_2-\kappa_1)}{\kappa_2+1}\left[\tfrac{1}{\xi(z)} + \bar{a}_1 \xi(z)\right] + \tfrac{Y}{R} z \end{aligned}\right\} \quad (z \in S_3). \tag{41}$$

Note that in reaching Eq. (41) use has been made of Eq. (37).

2.2. Uniform stress state in anti-plane shear deformations

The anti-plane shear problem discussed here is similar to that addressed in Sect. 2.1 except that the three-phase composite is now loaded by remote uniform anti-plane shear stresses σ_{zx}^{∞} and σ_{zy}^{∞}.

In anti-plane shear deformations with $u = v = 0, w = w(x, y)$, the non-vanishing shear stresses σ_{zx} and σ_{zy}, displacement w, and traction t_z on a lateral boundary surface can be expressed in terms of a single analytic function $f(z) = f(\omega(\xi)) \equiv f(\xi)$ as (e.g., [9,22])

$$w = \frac{1}{\mu}\mathrm{Im}[f(\xi)], \quad \sigma_{zy} + i\sigma_{zx} = \frac{f'(\xi)}{\omega'(\xi)}, \quad t_z = -\frac{\mathrm{d}}{\mathrm{d}s}Re[f(\xi)], \tag{42}$$

where s is the arc length parameter along the boundary curve on a cross-section.

In order to achieve a uniform stress state within the inclusion $S_1, f_1(z)$ needs to have the following form:

$$f_1(z) = \frac{\Pi}{R}z, \tag{43}$$

where Π is a complex constant to be determined.

By enforcing the continuity conditions of tractions and displacements across the two perfectly bonded interfaces L_1 and L_2 and using the analytic continuation method, the analytic function in the interphase layer and in the matrix can be determined to be

$$f_2(\xi) = \frac{1+\Gamma_1}{2\Gamma_1}\Pi\left(\xi + \sum_{n=1}^{N}\frac{a_n}{\xi^n}\right) - \frac{1-\Gamma_1}{2\Gamma_1}\bar{\Pi}\left(\frac{1}{\xi} + \sum_{n=1}^{N}\bar{a}_n\xi^n\right) \quad \left(1 < |\xi| < \rho^{-\frac{1}{2}}\right), \tag{44}$$

$$\begin{aligned} f_3(\xi) = {} & \frac{\Pi(1+\Gamma_1)(1+\Gamma_3)}{4\Gamma_1}\left(\xi + \sum_{n=1}^{N}\frac{a_n}{\xi^n}\right) - \frac{\bar{\Pi}(1-\Gamma_1)(1+\Gamma_3)}{4\Gamma_1}\left(\frac{1}{\xi} + \sum_{n=1}^{N}\bar{a}_n\xi^n\right) \\ & + \frac{\bar{\Pi}(1+\Gamma_1)(1-\Gamma_3)}{4\Gamma_1}\left(\frac{1}{\rho\xi} + \sum_{n=1}^{N}\bar{a}_n\rho^n\xi^n\right) - \frac{\Pi(1-\Gamma_1)(1-\Gamma_3)}{4\Gamma_1}\left(\rho\xi + \sum_{n=1}^{N}\frac{a_n}{\rho^n\xi^n}\right) \quad \left(|\xi| > \rho^{-\frac{1}{2}}\right), \end{aligned} \tag{45}$$

where $\Gamma_1 \equiv \mu_1/\mu_2$ and $\Gamma_3 \equiv \mu_3/\mu_2$, which are the same as those used in Sect. 2.1 for the in-plane loading case. Note that in reaching Eqs. (44) and (45) use has been made of Eqs. (42), (43), and (3).

In order to satisfy the remote asymptotic condition of

$$f_3(\xi) \cong R\left(\sigma_{zy}^{\infty} + i\sigma_{zx}^{\infty}\right)\xi + O(1) \quad \text{as} \quad |\xi| \to \infty, \tag{46}$$

the conformal mapping function $\omega(\xi)$ also has the form given in Eq. (36). This identified inclusion shape (as characterized by Eq. (36)) with uniform stresses in the inclusion is in agreement with that provided in [1] for generating a uniform stress state inside an inclusion bonded to a surrounding matrix through a 'spring-layer type' imperfect interface with vanishing thickness.

Also, it follows from Eqs. (36), (45), and (46) that the thickness parameter ρ is given by

$$\rho = \left[\frac{(1-\Gamma_1)(1+\Gamma_3)}{(1+\Gamma_1)(1-\Gamma_3)}\right]^{\frac{1}{N}} \ (N \geq 2) \tag{47}$$

and the constant Π satisfies

$$\begin{aligned} & \Pi\left[(1+\Gamma_1)(1+\Gamma_3) - \rho(1-\Gamma_1)(1-\Gamma_3)\right] + \bar{\Pi}\bar{a}_1\left[\rho(1+\Gamma_1)(1-\Gamma_3) - (1-\Gamma_1)(1+\Gamma_3)\right] \\ & \quad = 4R\Gamma_1(\sigma_{zy}^{\infty} + i\sigma_{zx}^{\infty}). \end{aligned} \tag{48}$$

For ρ determined from Eq. (47) to satisfy the condition of $0 \leq \rho \leq 1$, it is required that

$$\mu_2 < \mu_1 < \mu_3 \text{ or } \mu_2 > \mu_1 > \mu_3, \tag{49}$$

which places a constraint on the shear moduli μ_1, μ_2, and μ_3.

Clearly, Eq. (48) shows that the constant Π can always be obtained for given material parameters Γ_1 and Γ_2 and remote uniform shear stresses σ_{zx}^{∞} and σ_{zy}^{∞}, thereby indicating that in anti-plane shear deformations the stresses inside the inclusion are unconditionally uniform.

From Eqs. (43)–(45), (3), and (36), the analytic functions in the physical z-plane for the current anti-plane shear problem can be expressed as, with the help of Eq. (4),

$$f_1(z) = \frac{\Pi}{R} z \quad (z \in S_1), \tag{50}$$

$$f_2(z) = \frac{\Pi(1+\Gamma_1)}{2R\Gamma_1} z - \frac{\bar{\Pi}(1-\Gamma_1)}{2\Gamma_1} \left\{ \frac{1}{\xi(z)} + \bar{a}_1 \xi(z) + \bar{a}_N \left[\xi(z)\right]^N \right\} \quad (z \in S_2), \tag{51}$$

$$\begin{aligned} f_3(z) = {} & \frac{\Pi(1+\Gamma_1)(1+\Gamma_3)}{4R\Gamma_1} z - \frac{\bar{\Pi}(1-\Gamma_1)(1+\Gamma_3)}{4\Gamma_1} \left[\frac{1}{\xi(z)} + \bar{a}_1 \xi(z) \right] \\ & + \frac{\bar{\Pi}(1+\Gamma_1)(1-\Gamma_3)}{4\Gamma_1} \left[\frac{1}{\rho\xi(z)} + \bar{a}_1 \rho \xi(z) \right] \\ & - \frac{\Pi(1-\Gamma_1)(1-\Gamma_3)}{4\Gamma_1} \left\{ \rho\xi(z) + \frac{a_1}{\rho\xi(z)} + \frac{a_N}{\rho^N \left[\xi(z)\right]^N} \right\} \quad (z \in S_3). \end{aligned} \tag{52}$$

Note that in reaching Eq. (52) use has been made of Eq. (47).

3. Conclusions

In this study, the existence of a uniform hydrostatic stress state inside a 2-D elastic inclusion bonded to a uniformly loaded infinite elastic matrix through an interphase layer is demonstrated for in-plane loading. It is shown that such a uniform hydrostatic stress field within the inclusion in the three-phase composite can be achieved by properly designing the inclusion shape, the elastic constants of the composite phases, and the thickness of the interphase layer. Three types of possible (non-elliptical) shapes of such inclusions are found, and two conditions that ensure a uniform hydrostatic stress state are derived for each type. The first condition links the interphase layer thickness to elastic properties of the composite phases, and the second relates the remote stresses to geometrical and material parameters of the three-phase composite.

Possible inclusion shapes and related conditions for generating a uniform stress field inside an elastic inclusion in a three-phase composite loaded by remote constant anti-plane shear stresses are also identified by following similar procedures.

Solutions of elementary forms are derived for several cases—both general and specific—which satisfy these conditions and involve either in-plane or anti-plane shear loading.

Acknowledgments

The work reported here is partially funded by a grant from the U.S. National Science Foundation (NSF), with Dr. Clark V. Cooper as the program manager, and by a MURI grant from the U.S. Air Force Office of Scientific Research (AFOSR), with Dr. David Stargel as the program manager. The support from these two programs is gratefully acknowledged by XLG. Also, the funding from ECUST in support of the current work is greatly appreciated by XW. Finally, the authors wish to thank Professor David Steigmann and an anonymous reviewer for their encouragements and helpful comments.

Appendix A: Harmonic elastic inclusions of arbitrary shape

Consider an arbitrary-shape elastic inclusion S_1 bonded to an infinite elastic matrix S_2 through a perfect interface L. The inclusion S_1 is called *harmonic* if the uniformity of the mean stress in the matrix S_2 remains unperturbed after S_1 is embedded.

In order to make the inclusion harmonic, the stress field within the inclusion needs to be uniform and hydrostatic. By enforcing the traction and displacement continuity conditions on the interface L, it can be shown that the two analytic functions $\phi_1(z), \psi_1(z)$ in the inclusion (with the shear modulus μ_1) and the two analytic functions $\phi_2(z), \psi_2(z)$ in the matrix (with the shear modulus μ_2) will have the following forms:

$$\phi_1(z) = \frac{A\Gamma(\kappa_2+1)}{2\Gamma+\kappa_1-1}z, \quad \psi_1(z) = 0 \quad (z \in S_1), \tag{A1}$$

$$\phi_2(z) = Az, \quad \psi_2(z) = \frac{2A\left[\Gamma(\kappa_2-1)-\kappa_1+1\right]}{2\Gamma+\kappa_1-1}D(z) \quad (z \in S_2), \tag{A2a,b}$$

where $\Gamma \equiv \mu_1/\mu_2, A$ is a real constant, and $D(z) = \bar{z}$ for $z \in L$ and is analytic outside L except at infinity, where it exhibits the following asymptotic behavior:

$$D(z) \to P(z) + O(1) \quad \text{as} \quad |z| \to \infty, \tag{A3}$$

with $P(z)$ being a polynomial in z [18]. Combining Eqs. (A2b) and (A3) gives

$$\psi_2(z) = \frac{2A\left[\Gamma(\kappa_2-1)-\kappa_1+1\right]}{2\Gamma+\kappa_1-1}P(z) + O(1) \quad \text{as} \quad |z| \to \infty. \tag{A4}$$

From Eqs. (2) and (A1) it follows that

$$\sigma_{xx}^{(1)} = \sigma_{yy}^{(1)} = \frac{2A\Gamma(\kappa_2+1)}{2\Gamma+\kappa_1-1}, \quad \sigma_{xy}^{(1)} = 0 \quad (z \in S_1), \tag{A5}$$

which show that the stress field inside the inclusion S_1 is indeed uniform and hydrostatic.

Using Eqs. (2), (A2a), and (A4) yields

$$\sigma_{xx}^{(2)} + \sigma_{yy}^{(2)} = 4A \quad (z \in S_2), \tag{A6}$$

which says that the mean stress does remain uniform (constant) anywhere in the matrix S_2 in the presence of the inclusion S_1.

Furthermore, it can be shown from Eqs. (A5), (A6) and the relations $\sigma_{xx}^{(2)}+\sigma_{yy}^{(2)} = \sigma_{nn}^{(2)}+\sigma_{tt}^{(2)}, \sigma_{nn}^{(2)} = \sigma_{nn}^{(1)}$ on L that the hoop stress is constant along the entire interface L (on the matrix side) and is given by

$$\sigma_{tt}^{(2)} = \frac{2A\left[\Gamma(3-\kappa_2)+2(\kappa_1-1)\right]}{2\Gamma+\kappa_1-1} \quad (z \in L). \tag{A7}$$

As an example, when the interface L is described by the conformal mapping function:

$$z = \omega(\xi) = R\left(\xi + \frac{a_1}{\xi} + \frac{i\lambda}{\xi^2}\right) \quad (|\xi| = 1), \tag{A8}$$

where a_1 and λ are two real constants, the polynomial $P(z)$ can be determined as

$$P(z) = a_1 z - i\lambda z^2/R. \tag{A9}$$

From Eqs. (A2a), (A4), and (A9), it then follows that the remote stresses have the following forms:

$$\sigma_{xx}^{\infty} = N_1 - Ky, \quad \sigma_{yy}^{\infty} = N_2 + Ky, \quad \sigma_{xy}^{\infty} = -Kx, \tag{A10}$$

where N_1, N_2, and K are three real constants given by

$$N_1 \equiv 2A\left[1-\frac{\Gamma(\kappa_2-1)+1-\kappa_1}{2\Gamma+\kappa_1-1}a_1\right], \quad N_2 \equiv 2A\left[1+\frac{\Gamma(\kappa_2-1)+1-\kappa_1}{2\Gamma+\kappa_1-1}a_1\right],$$
$$K \equiv \frac{4A\lambda\left[\Gamma(\kappa_2-1)+1-\kappa_1\right]}{R(2\Gamma+\kappa_1-1)}, \tag{A11}$$

with A, a_1 and λ being three real constants to be determined from the inclusion shape. Clearly, Eq. (A10) shows that the remote stresses needed for making the inclusion harmonic have to be linearly distributed (rather than uniform).

Conversely, for given remote (non-uniform) stresses (with the restriction that the mean stress is constant), the polynomial $P(z)$ can be determined from the far-field boundary conditions using Eqs. (2), (A2a), and (A4). The shape of the harmonic inclusion described by $z=\omega(\xi)(|\xi|=1)$ can then be obtained from $P(z)$ using Eq. (A3). It should be pointed out that the non-uniform loading discussed here is different from that considered in [3].

Appendix B: Expressions of $\phi_3(\xi)$ and $\psi_3(\xi)$

When $N=2$, $\phi_3(\xi)$ and $\psi_3(\xi)$ can be obtained from Eqs. (16), (17) and (3) as

$$\begin{aligned}
\phi_3(\xi) &= \frac{X(2\Gamma_1+\kappa_1-1)\left[\Gamma_3(\kappa_2-1)+2\right]}{\Gamma_1(\kappa_2+1)(\kappa_3+1)}\left(\xi+\frac{a_1}{\xi}+\frac{a_2}{\xi^2}\right) \\
&\quad+\frac{2X(1-\Gamma_3)\left[\Gamma_1(\kappa_2-1)+1-\kappa_1\right]}{\Gamma_1(\kappa_2+1)(\kappa_3+1)}\left(\rho\xi+\frac{a_1}{\rho\xi}+\frac{a_2}{\rho^2\xi^2}\right), \\
\psi_3(\xi) &= \frac{2\bar{a}_1X\left\{(\Gamma_3+\kappa_3)\left[\Gamma_1(\kappa_2-1)+1-\kappa_1\right]+\rho(2\Gamma_1+\kappa_1-1)\left[(\kappa_3-1)-\Gamma_3(\kappa_2-1)\right]\right\}}{\Gamma_1(\kappa_2+1)(\kappa_3+1)}\xi \\
&\quad+\frac{2X\left\{(2\Gamma_1+\kappa_1-1)\left[(\kappa_3-1)-\Gamma_3(\kappa_2-1)\right]+\rho(\Gamma_3+\kappa_3)\left[\Gamma_1(\kappa_2-1)+1-\kappa_1\right]\right\}}{\Gamma_1(\kappa_2+1)(\kappa_3+1)}\frac{1}{\rho\xi} \\
&\quad+\frac{2X(1-\Gamma_3)\left[\Gamma_1(\kappa_2-1)+1-\kappa_1\right]\left\{(\bar{a}_1+\bar{a}_2\rho\xi)\left(a_1-\rho^2\xi^2+\frac{2a_2}{\rho\xi}\right)-1+\frac{a_1}{\rho^2\xi^2}+\frac{2a_2}{\rho^3\xi^3}\right\}}{\Gamma_1(\kappa_2+1)(\kappa_3+1)\left(\xi-\frac{a_1}{\xi}-\frac{2a_2}{\xi^2}\right)}
\end{aligned} \tag{B1}$$

for $|\xi|>\rho^{-\frac{1}{2}}$.

When $N=3$, $\phi_3(\xi)$ and $\psi_3(\xi)$ can be determined from Eqs. (16), (18) and (3) as

$$\begin{aligned}
\phi_3(\xi) &= \frac{X(2\Gamma_1+\kappa_1-1)\left[\Gamma_3(\kappa_2-1)+2\right]}{\Gamma_1(\kappa_2+1)(\kappa_3+1)}\left(\xi+\frac{a_1}{\xi}+\frac{a_3}{\xi^3}\right) \\
&\quad+\frac{2X(1-\Gamma_3)\left[\Gamma_1(\kappa_2-1)+1-\kappa_1\right]}{\Gamma_1(\kappa_2+1)(\kappa_3+1)}\left(\rho\xi+\frac{a_1}{\rho\xi}+\frac{a_3}{\rho^3\xi^3}\right), \\
\psi_3(\xi) &= \frac{2X\begin{pmatrix}\bar{a}_1(\Gamma_3+\kappa_3)\left[\Gamma_1(\kappa_2-1)+1-\kappa_1\right] \\ +\bar{a}_1\rho(2\Gamma_1+\kappa_1-1)\left[\kappa_3-1-\Gamma_3(\kappa_2-1)\right]\end{pmatrix}}{\Gamma_1(\kappa_2+1)(\kappa_3+1)}\xi \\
&\quad+\frac{2X\left\{(2\Gamma_1+\kappa_1-1)\left[\kappa_3-1-\Gamma_3(\kappa_2-1)\right]+\rho(\Gamma_3+\kappa_3)\left[\Gamma_1(\kappa_2-1)+1-\kappa_1\right]\right\}}{\Gamma_1(\kappa_2+1)(\kappa_3+1)}\frac{1}{\rho\xi} \\
&\quad+\frac{2X(1-\Gamma_3)\left[\Gamma_1(\kappa_2-1)+1-\kappa_1\right]\begin{pmatrix}-1+a_1\bar{a}_1+3a_3\bar{a}_3+(a_1\bar{a}_3-\bar{a}_1)\rho^2\xi^2-\bar{a}_3\rho^4\xi^4 \\ +\frac{a_1+3\bar{a}_1a_3}{\rho^2\xi^2}+\frac{3a_3}{\rho^4\xi^4}\end{pmatrix}}{\Gamma_1(\kappa_2+1)(\kappa_3+1)\left(\xi-\frac{a_1}{\xi}-\frac{3a_3}{\xi^3}\right)}
\end{aligned} \tag{B2}$$

for $|\xi| > \rho^{-\frac{1}{2}}$.

When $N \geq 4, \phi_3(\xi)$ and $\psi_3(\xi)$ can be obtained from Eqs. (16), (19) and (3) as

$$\begin{aligned}
\phi_3(\xi) &= \frac{X(2\Gamma_1+\kappa_1-1)\left[\Gamma_3(\kappa_2-1)+2\right]}{\Gamma_1(\kappa_2+1)(\kappa_3+1)}\left(\xi+\frac{a_N}{\xi^N}\right) \\
&\quad+\frac{2X(1-\Gamma_3)\left[\Gamma_1(\kappa_2-1)+1-\kappa_1\right]}{\Gamma_1(\kappa_2+1)(\kappa_3+1)}\left(\rho\xi+\frac{a_N}{\rho^N\xi^N}\right), \\
\psi_3(\xi) &= \frac{2X\left\{(2\Gamma_1+\kappa_1-1)\left[(\kappa_3-1)-\Gamma_3(\kappa_2-1)\right]+\rho(\Gamma_3+\kappa_3)\left[\Gamma_1(\kappa_2-1)+1-\kappa_1\right]\right\}}{\Gamma_1(\kappa_2+1)(\kappa_3+1)}\frac{1}{\rho\xi} \\
&\quad+\frac{2X\left\{\begin{array}{l}\bar{a}_N(2\Gamma_1+\kappa_1-1)\left[(\kappa_3-1)-\Gamma_3(\kappa_2-1)\right]\rho^N \\ +\bar{a}_N(\Gamma_3+\kappa_3)\left[\Gamma_1(\kappa_2-1)+1-\kappa_1\right]\end{array}\right\}}{\Gamma_1(\kappa_2+1)(\kappa_3+1)}\xi^N \\
&\quad+\frac{2X(1-\Gamma_3)\left[\Gamma_1(\kappa_2-1)+1-\kappa_1\right]\left[-1+Na_N\bar{a}_N-\bar{a}_N\rho^{N+1}\xi^{N+1}+\frac{Na_N}{\rho^{N+1}\xi^{N+1}}\right]}{\Gamma_1(\kappa_2+1)(\kappa_3+1)\left(\xi-\frac{Na_N}{\xi^N}\right)}
\end{aligned} \tag{B3}$$

for $|\xi| > \rho^{-\frac{1}{2}}$.

References

1. Antipov, Y.A., Schiavone, P.: On the uniformity of stresses inside an inhomogeneity of arbitrary shape. IMA J. Appl. Math. **68**, 299–311 (2003)
2. Bjorkman, G.S., Richards, R.: Harmonic holes—an inverse problem in elasticity. ASME J. Appl. Mech. **43**, 414–418 (1976)
3. Bjorkman, G.S., Richards, R.: Harmonic holes for nonconstant fields. ASME J. Appl. Mech **46**, 573–576 (1979)
4. Cherepanov, G.P.: Inverse problems of the plane theory of elasticity. J. Appl. Math. Mech. (PMM) **38**, 915–931 (1974)
5. Eshelby, J.D.: The determination of the elastic field of an ellipsoidal inclusion, and related problems. Proc. R. Soc. Lond. A **241**, 376–396 (1957)
6. England, A.H.: Complex Variable Methods in Elasticity. Wiley, London (1971)
7. Gao, C.F., Noda, N.: Faber series method for two-dimensional problems of an arbitrarily shaped inclusion in piezoelectric materials. Acta Mech. **171**, 1–13 (2004)
8. Gao, X.-L.: A general solution of an infinite elastic plate with an elliptic hole under biaxial loading. Int. J. Press. Vessels Pip. **67**, 95–104 (1996)
9. Gao, X.-L.: A mathematical analysis of the elasto-plastic anti-plane shear problem of a power-law material and one class of closed-form solutions. Int. J. Solids Struct. **33**, 2213–2223 (1996)
10. Gao, X.-L.: A mathematical analysis for the plane stress problem of a power-law material. IMA J. Appl. Math. **60**, 139–149 (1998)
11. Gao, X.-L.: On the complex variable displacement method in plane isotropic elasticity. Mech. Res. Commun. **31**, 169–173 (2004)
12. Gao, X.-L., Ma, H.M.: Strain gradient solution for Eshelby's ellipsoidal inclusion problem. Proc. R. Soc. A **466**, 2425–2446 (2010)
13. Hardiman, N.J.: Elliptic elastic inclusion in an infinite elastic plate. Q. J. Mech. Appl. Math. **7**, 226–230 (1954)
14. Luo, J.-C., Gao, C.-F.: Stress field of a coated arbitrary shape inclusion. Meccanica (2010). doi:10.1007/s11012-010-9363-3
15. Markenscoff, X.: Inclusions with constant eigenstress. J. Mech. Phys. Solids **46**, 2297–2301 (1998)
16. Muskhelishvili, N.I.: Some Basic Problems of the Mathematical Theory of Elasticity. P. Noordhoff, Groningen, The Netherlands (1953)
17. Ru, C.Q.: Three-phase elliptical inclusions with internal uniform hydrostatic stresses. J. Mech. Phys. Solids **47**, 259–273 (1999)
18. Ru, C.Q.: Analytical solution for Eshelby's problem of an inclusion of arbitrary shape in a plane or half-plane. ASME J. Appl. Mech. **66**, 315–322 (1999)
19. Ru, C.Q., Schiavone, P., Mioduchowski, A.: Uniformity of stresses within a three-phase elliptic inclusion in anti-plane shear. J. Elast. **52**, 121–128 (1999)
20. Sadd, M.H.: Elasticity: Theory, Applications, and Numerics. 2nd edn. Academic Press, Burlington, MA (2009)
21. Sendeckyj, G.P.: Elastic inclusion problems in plane elastostatics. Int. J. Solids Struct. **6**, 1535–1543 (1970)

22. Slaughter, W.S.: The Linearized Theory of Elasticity. Birkhäuser, Boston (2002)
23. Tsukrov, I., Novak, J.: Effective elastic properties of solids with two-dimensional inclusions of irregular shape. Int. J. Solids Struct. **41**, 6905–6924 (2004)
24. Wang, G.F., Schiavone, P., Ru, C.Q.: Harmonic shapes in finite elasticity under nonuniform loading. ASME J. Appl. Mech. **72**, 691–694 (2005)
25. Wang, X.: Eshelby's problem of an inclusion of arbitrary shape in a decagonal quasicrystalline plane or half-plane. Int. J. Eng. Sci. **42**, 1911–1930 (2004)
26. Wang, X.: Three-phase elliptical inclusions with internal uniform hydrostatic stresses in finite plane elastostatics. Acta Mech. **219**, 77–90 (2011)
27. Wheeler, L.T.: Stress minimum forms for elastic solids. Appl. Mech. Rev. **45**, 1–11 (1992)
28. Zou, W.N., He, Q.-C., Huang, M.J., Zheng, Q.-S.: Eshelby's problem of non-elliptical inclusions. J. Mech. Phys. Solids **58**, 346–372 (2010)

X. Wang
School of Mechanical and Power Engineering
East China University of Science and Technology
130 Meilong Road
Shanghai 200237
China

X.-L. Gao
Department of Mechanical Engineering
Texas A&M University
3123 TAMU
College Station, TX 77843-3123
USA
e-mail: xlgao@tamu.edu

(Received: February 4, 2011; revised: May 4, 2011)